Quantitative estimation of concentrations of dissolved rare earth elements using reflectance spectroscopy

Jingjing Dai
Denghong Wang
Runsheng Wang
Zhenghui Chen

Quantitative estimation of concentrations of dissolved rare earth elements using reflectance spectroscopy

Jingjing Dai,[a] Denghong Wang,[a] Runsheng Wang,[b] and Zhenghui Chen[a]

[a]MLR Key Laboratory of Metallogeny and Mineral Assessment, Institute of Mineral Resources, CAGS, Beijing 100037, China
daijingjing863@sina.com

[b]China Aero Geophysical Survey & Remote Sensing Center for Land and Resources, Beijing 100083, China

Abstract. Characteristic spectral parameters such as the wavelength and depth of absorption bands are widely used to quantitatively estimate the composition of samples from hyperspectral reflectance data in soil science, mineralogy as well as vegetation study. However, little research has been conducted on the spectral characteristic of rare earth elements (REE) and their relationship with chemical composition of aqueous solutions. Reflectance spectra of ore leachate solutions and contaminated stream water from a few REE mines in the Jiangxi Province, China, are studied for the first time in this work. The results demonstrate that the six diagnostic absorption features of the rare earths are recognized in visible and near-infrared wavelengths at 574, 790, 736, 520, 861, and 443 nm. The intensity of each of these six absorption bands is linearly correlated with the abundance of total REE, with the r^2 value >0.95 and the detection limit at ≥75,000 μg/L. It is suggested that reflectance spectroscopy provides an ideal routine analytical tool for characterizing leachate samples. The outcome of this study also has implications for monitoring the environmental effect of REE mining, in particular in stream water systems by hyperspectral remote sensing. © *The Authors. Published by SPIE under a Creative Commons Attribution 3.0 Unported License. Distribution or reproduction of this work in whole or in part requires full attribution of the original publication, including its DOI.* [DOI: 10 .1117/1.JRS.7.073513]

1 Introduction

Rare earths are valuable resources that play an important role in modern industrial materials. Weathered crust rare earth ore is a new type of rare earth resource in China, which was first discovered in Jiangxi and later found widely in south China. This type of rare earth ore has many advantages, such as wide distribution, huge reserve, low radioactivity, and easy extraction.[1] In weathered crust rare earth ores, the rare earth ions are absorbed in clay minerals formed from weathering of granites and volcanic rocks.[2] Thus the rare earths can be easily extracted by an ion-exchange method. In the metallurgical process, the rare earth elements (REE) absorbed in clay minerals are dissolved in ammonia sulfate solution, which are collected in a leaching liquor pool. Then rare earths are deposited by carbonic acid solution.[1,3] Nowadays, unauthorized mining of weathered crust rare earth ores becomes more and more serious as the price of rare earths is rising. The leaching liquor pools that contain different concentrations of dissolved rare earths are discharged arbitrarily. Thus, the rivers near rare earth ores are often polluted by discharge or groundwater permeation of leaching liquor, which lead to severe changes of elemental balance in the environment and the biosphere, which in turn, have the potential to endanger public health.[4–6]

The concentration of dissolved REE is a vital factor to evaluate the abundance of REE in leaching liquor and to estimate the contamination of the river near the rare earth ores. Conventionally, quantitative measurement of the abundance of REE in aqueous solutions is

done by laboratory-based analytical techniques, such as the inductively coupled plasma mass spectrometry (ICP-MS),[7] which are time consuming and costly. Consequently, a simple and economic method is necessary for measuring the content of REE in aqueous media. Reflectance spectroscopy is a rapidly advancing technique used to acquire spectral reflectance data in the visible-near infrared (VNIR) and short-wave infrared (SWIR) wavelength regions (0.4 to 2.5 nm) for material characterization.[8,9] The spectral reflectance method as an analytical tool has advantages such as rapid data acquisition, nondestructive sample measurement, and low operational cost.[10–12] Electronic transition and charge transfer processes associated with transition metal ions cause absorptions of incident light in the visible and infrared region, producing diagnostic spectral features.[13–16] Previous studies have established that the absorption bands in the visible wavelength region related to REE are due to electronic transitions within the 4f configuration.[17–20] It has been found that the wavelength, shape, depth, and width of the absorption features are controlled by the chemical composition of the material. Therefore, the variation of absorption features can be directly related to the chemistry of the absorbing material, for instance, the depth of an absorption band is an indication for the amount of the absorbing material present in a sample.[16,21,22] Reflectance spectra acquired in the field and laboratory have been used to retrieve the chemical composition of samples in soil science and geology as well as botany.[23–31] However, little research has been undertaken on the diagnostic absorption features of REE, and few data have been published on the relationship between absorption features and chemical composition of REE. Of the few available references in the literature, Clark et al. showed the spectral characteristics of several rare earth oxides involving Eu, Nd, and Sm,[32] and Rowan et al. and Bedini identified the absorption bands of REE at 0.58, 0.74, and 0.80 μm which are attributed to electronic transitions of Nd^{3+} in REE-bearing minerals.[33,34] Silver et al. showed the spectral characteristics of yttrium oxides doped with different contents of Nd, Er, and Ho.[35]

In this paper, we present a new method for quantitative estimation of the concentration of REE dissolved in aqueous media using reflectance spectroscopy. In our study, pure water, rare earth oxide, and ore leaching liquor samples containing various amounts of REE were collected; the reflectance spectra and the concentrations of REE were measured by reflectance spectroscopy and ICP-MS, respectively. Then, the spectrally diagnostic absorption characteristics of these samples were analyzed, and the lower detection limit by the spectral absorption band method for REE in aqueous media was determined. Finally, the correlation between the spectral absorption depth and the concentration of REE was analyzed, and linear regression models were derived that can be used for estimating the concentration of REE in aqueous media samples.

2 Samples and Methods

2.1 Sample Collection

In this study, 10 leaching liquor and stream water specimens numbered D1 to D10 which contain different concentrations of REE were collected from three rare earth ores in Xunwu, Dingnan, and Anyuan, respectively, in southern Jiangxi in May 2012 (Figs. 1 and 2). In this study, samples were collected and stored in high-density polyethylene bottles. The samples were then filtered through 0.45-μm membranes to remove suspended substances. The filtered samples were kept in a cold storage at temperatures between 0℃ and 4℃ before spectral reflectance and chemical measurements.

2.2 Spectral Reflectance Measurements

The spectral reflectance data of the aqueous samples were acquired using ASD FieldSpec-3 portable spectroradiometer in a darkroom. The FieldSpec-3 spectroradiometer measures dispersive reflectance at wavelengths from 0.35 to 2.5 μm which contains the wavelengths of diagnostic electronic transitions of REE (Table 1).[36] The setup of spectral reflectance measurement is illustrated in Fig. 3. A large sheet of white paper was placed on the table to form a diffuse reflection surface. Then, 40 ml of each sample was poured into a clean beaker (50 ml capacity)
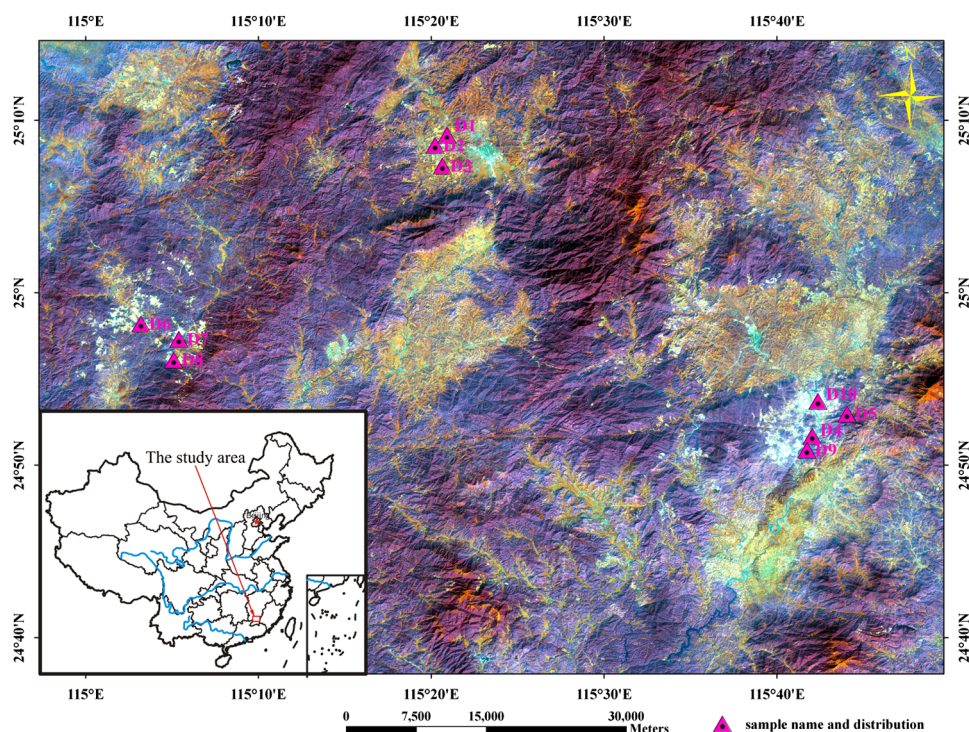
Fig. 1 The distribution of samples on Landsat ETM 532 band composition image. The white areas on the image present the rare earth mining areas and our samples distribute in three different rare earth ores in south Jiangxi province of China.
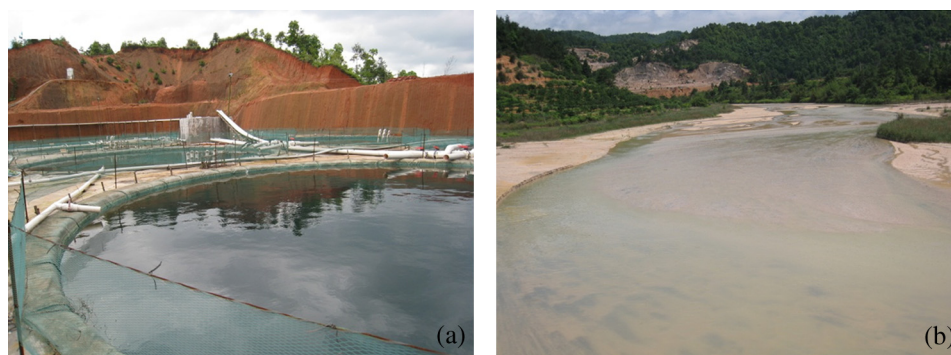

Fig. 2 Samples collected in the leaching liquor pools (a) and in the rivers which are polluted by the neighboring rare earth ores (b).

placed on the table. Tripods were used for holding the lamp and the sensor. The positions of the lamp, the foreoptical lens of the ASD spectroradiometer, and the beaker remained constant for all samples measured to ensure each sample was measured under exactly the same geometric condition. For reference, a Spectralon$^{@}$ plate was measured in the same position as the beaker. An 8 deg field-of-view foreoptics lens was used for spectral data acquisition. The incident angle of light source was 30 deg, for the luminous beams point to the beaker, while the foreoptics lens was placed perpendicular above the beaker. The distance from the lamp to the center of the liquid surface in the beaker was 10 cm, while the range from the lens to the liquid surface was 8 cm.

Spectral reflectance measurements were undertaken using ASD built-in software (ASD ViewSpecPro). Spectral reflectance of samples was measured in reference to Spectralon. Five spectral scans were repeated for each sample and an average spectrum was recorded. For comparison of the reflectance spectra of samples containing different concentrations of REE, reflectance spectra of pure water and rare earth oxides were measured.

Table 1 Details of the ASD FieldSpec-3 spectroradiometer.

Spectral range	350 to 2500 nm
Detectors	VNIR (350 to 1000 nm)
	SWIR1 (1000 to 1830 nm)
	SWIR2 (1830 to 2500 nm)
Spectral resolution	3 nm at 700 nm
	10 nm at 1400 nm
	10 nm at 2100 nm
Sampling interval	1.4 nm for 350 to 1000 nm
	2 nm for 1000 to 2500 nm
Field of view	8, 18, 28 deg
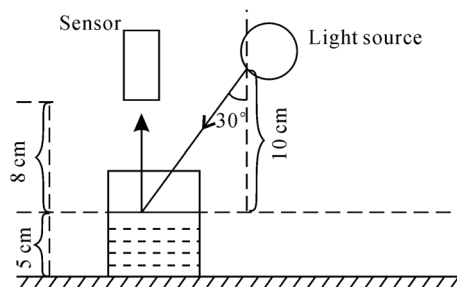
Fig. 3 General setting for laboratory measurements with ASD FieldSpec-3 spectroradiometer.

Continuum removal was undertaken as a pre-processing procedure. This is based on the assumption that an absorption spectrum has two components: a continuum and individual absorption features. The continuum or background is the overall albedo of the reflectance curve. To remove the background, continuum was fitted to a raw spectrum and at each wavelength the reflectance was divided by this continuum.[37,38] Mathematically this was done as follows: $R_{cc}(w) = R(w)/R_c(w)$, where $R(w)$ is the spectrum as a function of wavelength w, R_c is the continuum for the spectrum, and R_{cc} is the continuum removal spectrum. For each absorption feature, we choose 10 nm as the wavelength range when performing continuum removal. Taking the absorption feature at 790 nm as an example, we used the 785 to 795 nm wavelength range for local continuum removal. Then the depth of the absorption feature, defined as the reflectance value at the shoulders minus the reflectance value at the absorption-band minimum, was calculated from continuum removal spectra as $D = 1 - R_b/R_c$, where R_b is the reflectance at the band bottom and R_c is the reflectance of the continuum at the same wavelength as R_b.[39]

2.3 Chemical Analyses

The concentrations of dissolved REE were measured using the ICP-MS in the National Research Center for Geoanalysis of China. The REE was extracted with mixed extracting agents of di(2-ethylhexyl)phosphoric acid (HDEHP) and mono(2-ethylhexyl)phosphoric acid (H2MEHP).[7] The detection limits for the various isotopes of REE are 0.022 μg/L for ^{89}Y, 0.018 μg/L for ^{139}La, 0.028 μg/L for ^{140}Ce, 0.005 μg/L for ^{141}Pr, 0.076 μg/L for ^{146}Nd, 0.009 μg/L for ^{147}Sm, 0.002 μg/L for ^{151}Eu, 0.021 μg/L for ^{157}Gd, 0.002 μg/L for ^{159}Tb, 0.009 μg/L for ^{163}Dy, 0.003 μg/L for ^{165}Ho, 0.005 μg/L for ^{167}Er, 0.002 μg/L for ^{169}Tm, 0.003 μg/L

Table 2 Concentrations of REE in leachate samples analyzed by inductively coupled plasma mass spectrometry.

Sample name	La (µg/L)	Ce (µg/L)	Pr (µg/L)	Nd (µg/L)	Sm (µg/L)	Eu (µg/L)	Gd (µg/L)	Tb (µg/L)	Dy (µg/L)	Ho (µg/L)	Er (µg/L)	Tm (µg/L)	Yb (µg/L)	Lu (µg/L)	Y (µg/L)	∑REE (µg/L)
D1	251,800	5698	53,630	18,6100	45,210	9027	52,190	6725	39,640	8382	21,710	3141	18,340	2634	221,200	925,427
D2	150,900	3901	31,670	10,8200	26,690	5617	33,820	4580	26,430	5709	14,890	2155	12,480	1785	164,900	593,727
D3	90,360	2596	185,00	62,760	15,060	3404	22,470	3350	19,650	3979	10,750	1611	9026	1357	125,500	390,373
D4	168,900	50,800	18,310	50,460	8389	1312	10,410	1474	8125	1624	3903	576	2714	348	60,050	387,395
D5	50,040	7395	12,350	46,100	9846	611	7898	920	5482	984	2089	193	1497	142	22,150	167,697
D6	22,180	744	3732	12,930	2910	475	4045	521	3674	549	1830	172	1297	121	21,230	76,410
D7	15,410	1231	3308	11,150	2307	374	2301	307	1687	271	743	66.4	420	55.1	8542	48172.5
D8	10,130	766	1897	6722	1424	297	1672	238	1263	219	607	55.3	322	46.4	6883	32541.7
D9	5396	2531	1081	3069	535	63.2	856	72.1	332	58.3	161	17.1	105	14.6	1939	16230.3
D10	3546	2032	665	2378	348	34.4	513	46.5	210	36.1	97.4	10.3	62.7	8.61	1396	11384.01

for ^{173}Yb, and 0.0005 μg/L for ^{175}Lu. The analytical precision for the heavy REE and yttrium is 2% to 3%, respectively, and approximately 5% for the light REE. For each sample, the total concentration of the 15 REE was calculated (Table 2).

2.4 Statistical Analysis

In our study, Pearson's correlation, linear regression, and cluster analysis were utilized. The coefficient of determination (r^2) was selected as the standard for determining the application of absorption intensity for the measurement of the concentrations of REE. The coefficient of determination (r^2) between the intensity of six absorption bands and the abundance of total REE, r^2 between the intensity of 6 absorption bands, and 15 single REE were calculated. The least squares method was used to establish the linear regression equation, which was applied to quantitatively estimating the concentrations of dissolved REE using reflectance spectroscopy.[22] Cluster analysis is a statistical technique that sorts observations into similar sets or groups.[40] In our study, it was used to group the 15 REE into different groups according to their concentrations in 10 samples.

3 Results

3.1 The Spectral Characteristics of Dissolved REE

Based on the chemical analyses (Table 2), the sample D1, which contained the maximum amounts of REE, was selected, and its spectrum was compared with the spectra of pure water and rare earth oxide. For pure water, the high reflectance at 20% to 70% in the visible wavelengths is due to high transmission of visible light in water and the white background underneath the beaker. The reflectance is reduced sharply in the near-infrared (NIR) and SWIR regions because of strong absorption by water in these wavelengths. Two board absorption features at 780 and 950 nm are probably caused by the white paper background. In the spectra of rare earth oxide, absorption bands at wavelengths of 1400 and 1900 nm are related to hydrous minerals, and the several sharp absorption features on visible and NIR wavelengths are due to REE. The main spectral reflectance characteristics of ore leachate sample D1 are similar to pure water, i.e., with high reflectance in visible wavelengths but very low reflectance in the NIR and SWIR regions (Fig. 4). Besides, the diagnostic spectral reflectance features of sample D1 show six intense absorption bands in the visible and NIR wavelengths at 574, 790, 736, 520, 861, and 443 nm according to the absorption intensity, similar to the absorption features of the
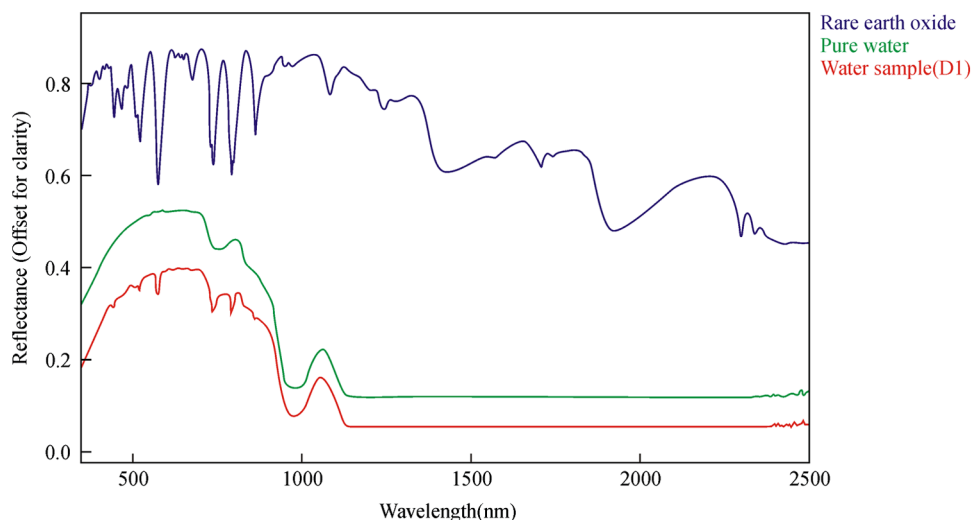

Fig. 4 The spectra of pure water, rare earth oxide, and leachate containing maximum concentration of total REE (D1).

rare earth oxides (Fig. 5). Furthermore, with the decrease in the concentrations of REE, i.e., from D1 to D10, the diagnostic absorption bands become weaker (Figs. 6 and 7). As revealed by the analysis of concentrations and absorption-band depth of the 10 samples, the upper five samples with higher concentrations of REE show well-developed diagnostic absorption characteristics. Therefore, the minimum concentration of total REE detectable by reflectance spectroscopy must exceed 75,000 μg/L.

3.2 Correlations Between the Concentration of Total REE and Diagnostic Absorption Features
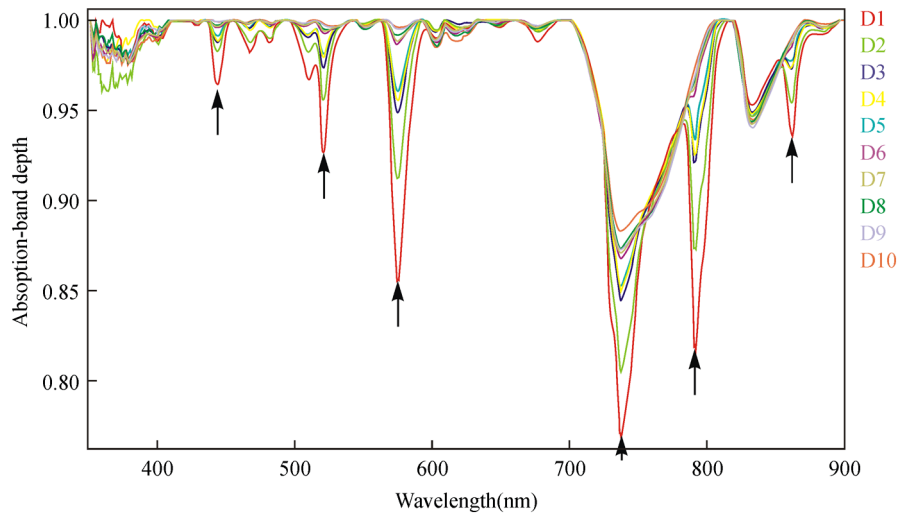
The relative intensity of the six diagnostic absorption features of REE was calculated on the local continuum removal spectra (Fig. 8). The relative depths of six diagnostic absorption features are listed in Table 3. A linear correlation model of relative absorption-band depth as a function of the concentration of total REE is established using the least squares method for each absorption feature (Fig. 9). The results show for each linear relationship the coefficient of determination (r^2) at about 0.96 to 0.97, e.g., the depth of the absorption feature has a high correlation with the concentrations of total REE. The
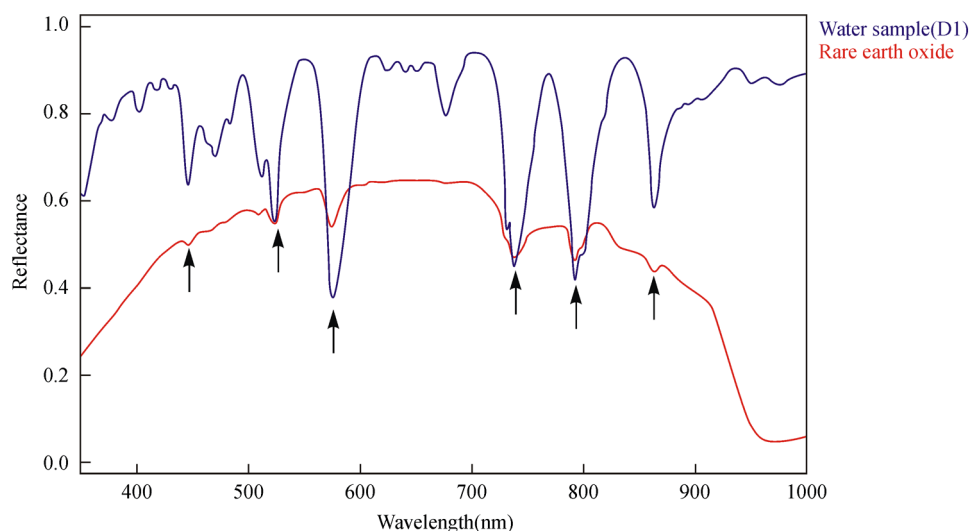

Fig. 5 The absorption feature of sample (D1) and pure rare earth oxide.
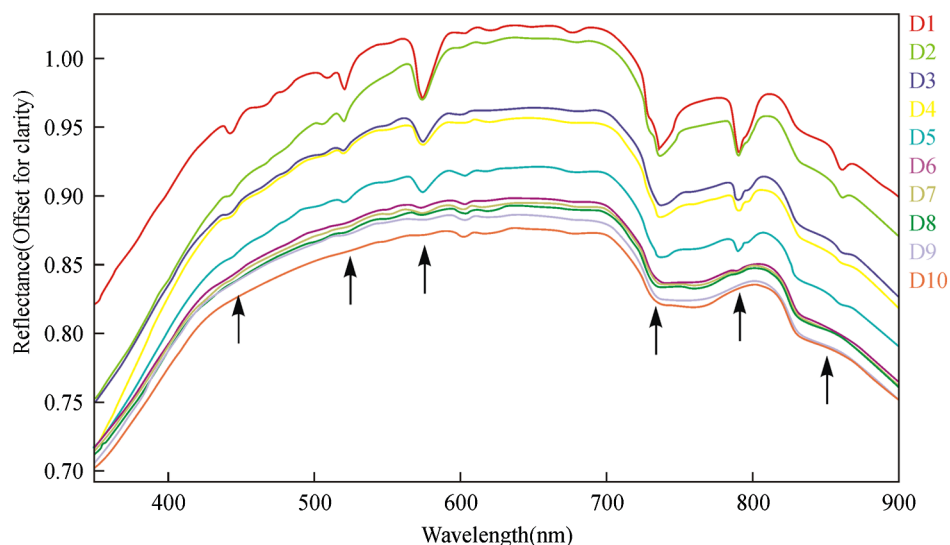
Fig. 6 The spectra of 10 samples that are listed from high to low according to the concentrations of total REE (wavelength from 350 to 900 nm).

Fig. 7 The spectra of 10 samples that are listed from high to low according to the concentrations of total REE (wavelength from 350 to 900 nm) after continuum removal.
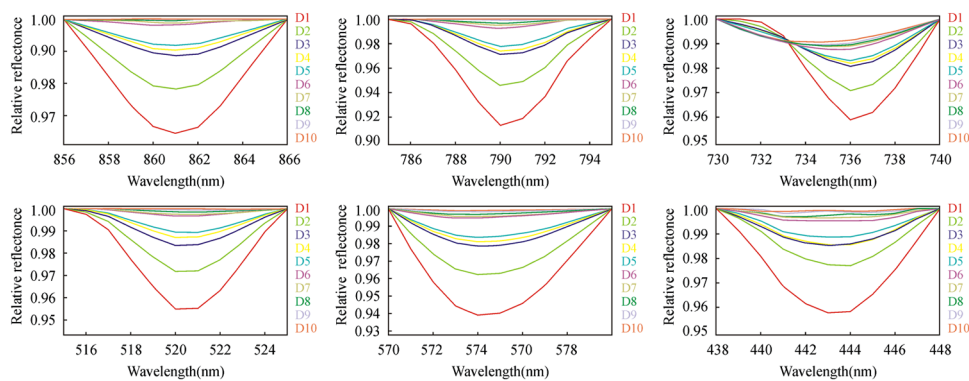
Fig. 8 The relative reflectance and depth on the six diagnostic absorption wavelengths for each sample.

linear regression equations for the absorption features at 574, 790, 736, 520, 861, and 443 nm are $y = 15.703x - 0.0057$, $y = 10.835x + 0.0088$, $y = 29.295x - 0.2549$, $y = 20.677x + 0.0128$, $y = 26.062x + 0.0293$, and $y = 40.092x - 0.016$, respectively. The standard error of prediction of the least squares method is 0.0511, 0.0526, 0.0588, 0.0470, 0.0538, and 0.0545 g/L for the absorption features at 574, 790, 736, 520, 862, and 443 nm, respectively.

3.3 Analysis of Correlation Between the Concentration of each Individual REE and Six Diagnostic Absorption Features

The REE contain 15 single elements; the correlation between concentration of each single element and the relative depths of six diagnostic absorption features was also analyzed using the linear regression method mentioned above. The results show that the 15 single elements can be divided into four groups according to the correlation coefficients (Table 4). The first group contains Ce, which has the lowest correlation coefficient of all four groups (<0.1). The second group is La, which has a correlation coefficient between 0.8 and 0.9. The third group contains Eu, Gd, Tb, Dy, Ho, Er, Tm, Yb, Lu, and Y, with correlation coefficients between 0.9 and 0.98. The fourth group contains Pr, Nd, and Sm, each with a correlation coefficient higher than 0.98.

For these 15 REE, cluster analysis was undertaken in reference to their concentrations (Table 2). The results also show that these elements are split into four groups (Fig. 10). Ce has little correlation with any other REE. La shows a low correlation with the rest of the REE. Eu, Gd, Tb, Dy, Ho, Er, Tm, Yb, Lu, Y form one closely correlated group, whereas
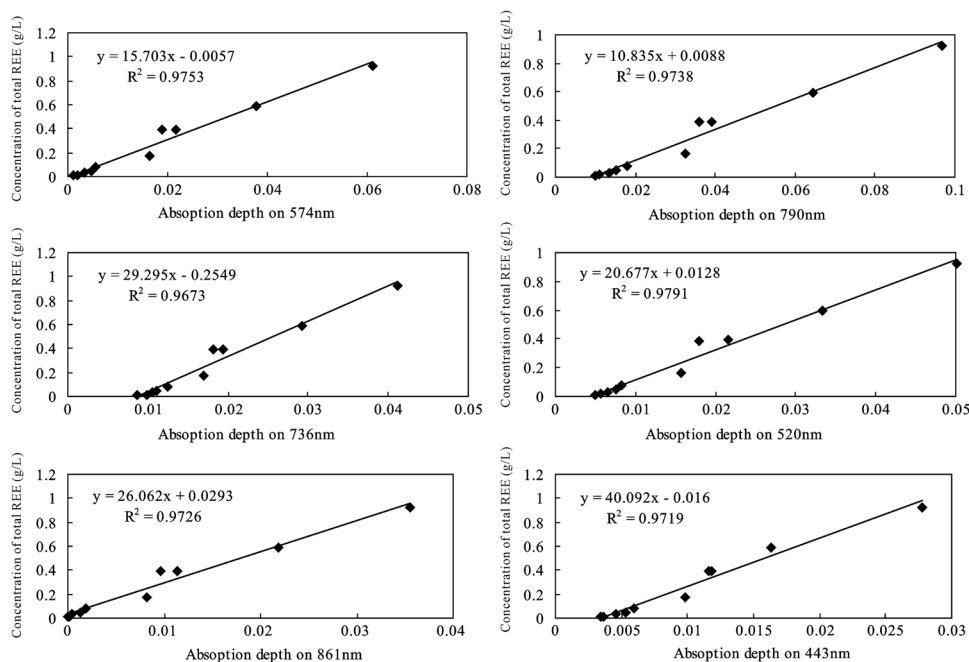
Table 3 The concentrations of total REE and the corresponding depths of six diagnostic absorption features.

Sample name	$\sum$REE (μg/L)	The depths on 574 nm	The depths on 790 nm	The depths on 736 nm	The depths on 520 nm	The depths on 862 nm	The depths on 443 nm
D1	925,427	0.06103	0.08671	0.04122	0.04524	0.03548	0.02472
D2	593,727	0.03782	0.05449	0.02923	0.0283	0.02182	0.01334
D3	390,373	0.02157	0.0291	0.01931	0.01656	0.01139	0.00879
D4	387,395	0.01902	0.02602	0.01811	0.01306	0.00963	0.00861
D5	167,697	0.01647	0.02244	0.01699	0.0107	0.00824	0.00678
D6	76,410	0.00542	0.00786	0.0124	0.00332	0.00191	0.0029
D7	48172.5	0.00468	0.00508	0.01113	0.0026	0.00128	0.00227
D8	32541.7	0.00334	0.00354	0.01055	0.00154	0.00045	0.0016
D9	16230.3	0.00187	0.00102	0.00984	0.00063	0.00021	0.00061
D10	11384.01	0.0011	0.00015	0.00868	0.0001	0.00002	0.00044

Pr, Nd, Sm form another well-correlated group. The results agree with the correlation analyses between the concentration of each individual element and the depth of its diagnostic absorption feature. Therefore, we can draw the conclusion that the chemical analysis and the spectral analysis can confirm one another.

4 Discussions and Conclusions

In this study, dissolved REE in aqueous media sampled from the leachate ponds and the nearby rivers were analyzed using reflectance spectroscopy with reference to pure water and synthesized rare earth oxide. It was observed that even though the concentration of REE in aqueous solution is very low,

Fig. 9 The linear regression of the concentration of total REE and absorption depth on six absorption wavelength features.

Table 4 The coefficient of determination (r^2) of the six diagnostic absorption features with the concentrations of the 15 individual REE.

	r^2 on 574 nm	r^2 on 790 nm	r^2 on 736 nm	r^2 on 520 nm	r^2 on 862 nm	r^2 on 443 nm
La	0.8777	0.8754	0.8632	0.8718	0.8684	0.8987
Ce	0.0145	0.0138	0.0097	0.0113	0.0111	0.0261
Pr	0.9966	0.9951	0.9916	0.9953	0.995	0.9938
Nd	0.9984	0.9971	0.9957	0.9973	0.9983	0.9912
Sm	0.988	0.9875	0.9895	0.9901	0.9911	0.9722
Eu	0.9509	0.9507	0.9553	0.9624	0.9577	0.9273
Gd	0.9703	0.9699	0.9707	0.9807	0.9743	0.9484
Tb	0.9536	0.9527	0.9515	0.9675	0.9566	0.9299
Dy	0.9526	0.9519	0.9514	0.9664	0.9556	0.9304
Ho	0.9522	0.9517	0.9516	0.9661	0.9566	0.926
Er	0.9377	0.9375	0.9383	0.9536	0.9425	0.9109
Tm	0.9262	0.9251	0.9248	0.9437	0.9315	0.899
Yb	0.9299	0.9296	0.9309	0.9466	0.9359	0.9011
Lu	0.9136	0.9123	0.9133	0.9321	0.92	0.8838
Y	0.924	0.9238	0.9207	0.9416	0.9265	0.8977
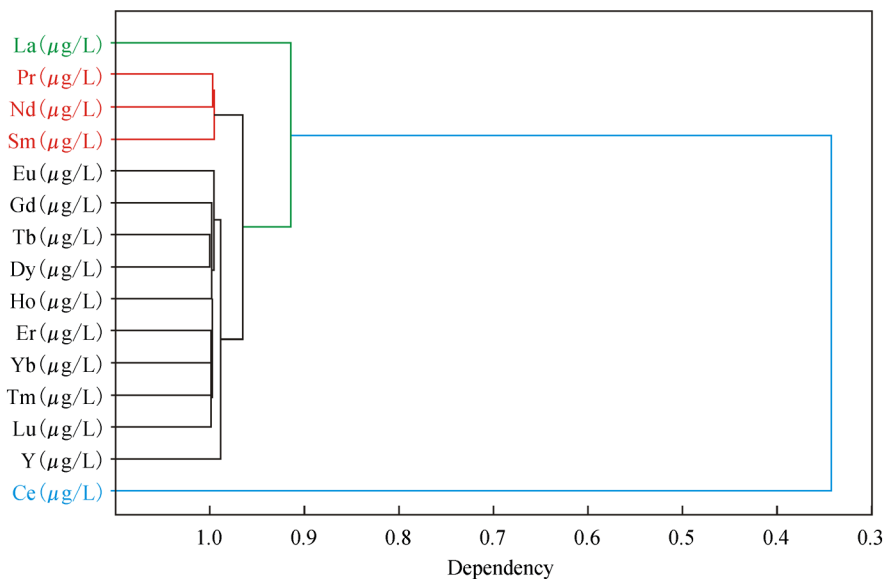
Fig. 10 Cluster analysis of the 15 individual REE according to their concentrations.

their spectral absorption features in visible and NIR wavelengths are detectable as shown by the six diagnostic absorption bands at 574, 790, 736, 520, 861, and 443 nm. Furthermore, with the descending of the REE concentration, the intensities of the six absorption features decrease. The minimum concentration of total REE that can be confidently detected by reflectance spectroscopy is approximately 75,000 μg/L. Thereafter, a linear correlation between the depth of each of the six diagnostic absorption features and the concentration of total REE has been found that can be used to estimate the concentration of total REE in ore leachate and river water samples. Based on the results of the

quantitative analyses in this study, it can be concluded that the relationship between the depth of the six diagnostic absorption features and the concentration of total REE can be quantified using a linear regression method at a high confidence level as indicated by the correlation coefficients up to 96% to 97%. The results of this study also show that the technique of using a linear relationship of absorption feature parameters for modeling the concentrations of REE is a simple first-order approximation. Furthermore, the study results in improved understanding of the reflectance spectroscopy of REE in liquid solutions, and bridges the gap between the reflectance spectroscopy of REE in aqueous media and their chemical concentration.

Based on the linear correlation between the diagnostic absorption features and the concentration of total REE, we can easily estimate the concentration of total REE with reflectance spectroscopy of aqueous samples. The ASD spectroradiometer can get 10 spectra/s in real time, and therefore the method stated in our paper can deal with massive samples in a short time. Currently, the reflectance spectroscopy can be obtained with portable spectroradiometer in fieldwork, which makes it possible to estimate the concentration of total REE without laboratory analysis. Therefore, our research could be used for routine monitoring of REE pollution as a quicker and cheaper method.

However, there are still questions remaining unanswered in this study, for which more research should be conducted:

1. Although the relationship between spectral responses and concentrations of REE shows a good linear correlation, the number of samples considered in this study is so limited as not to permit a thorough statistical analysis. Due to suspended mining operations, we could only obtained 10 leachate samples from three mines. More leachate samples will be collected when mining resumes in the near future.

2. In this study, total REE comprising 15 individual REE were studied with regard to their spectral characteristics in relation to the concentrations in liquid solution. It is necessary to carry out subsequent work to study the reflectance spectral characteristics of each individual REE or a subgroup of REE, such as the light REE or the heavy REE, and the relationship between spectral response and their chemical concentration.

3. In this study, the depth of an absorption band is used as a parameter for quantitative analysis. It may be worthwhile to test other spectral parameters such as second derivative as a concentration index for correlation analysis. Also, even though the liner regression method as used in this study has proven useful to provide a simple and reliable approximation for the concentration of REE, in a future study other modeling techniques need to be tested for modeling more complex relationships.

4. If field study is conducted using spectroradiometers, more research work needs to be done to refine this technique for routine monitoring, such as the study of the influence of sunlight, and the impacts of silt, chlorophyll, and heavy metals in water.

Acknowledgments

References

1. R. Chi and J. Tian, *Weathered Crust Rare Earth Ore: Chemistry and Metallurgy*, Science Publishing House, Beijing (2006).
2. R. Chi and J. Tian, "Review of weathered crust rare earth ore," *J. Chin. Rare Earth Soc.* **25**(6), 641–650 (2007).http://dx.doi.org/10.3321/j.issn:1000-4343.2007.06.001

3. Z. Gao and Q. Zhou, "Contamination from rare earth ore strip mining and its impacts on resources and eco-environment," *Chin. J. Ecol.* **30**(12), 2915–2922 (2011).

4. K. H. Johannesson et al., "Geochemistry of the rare-earth elements in hypersaline and dilute acidic natural terrestrial waters: complexation behavior and middle rare-earth element enrichments," *Chem. Geol.* **133**(1–4), 125–144 (1996), http://dx.doi.org/10.1016/S0009-2541(96)00072-1.

5. M. Åstrom, "Abundance and fractionation patterns of rare earth elements in streams affected by acid sulphate soils," *Chem. Geol.* **175**(3–4), 249–258 (2001), http://dx.doi.org/10.1016/S0009-2541(00)00294-1.

6. B. Yan, H. Huang, and X. Xiao, "Technology analysis for resource recycles and standardized discharge of ion-absorbed rare earth mineral wastewater," *Chin. J. Environ. Eng.* **4**(1), 53–56 (2010).

7. G. Han and C. Liu, "Controlling factors for variation in dissolved rare-earth elements in Karst drainage basin," *Carsol. Sin.* **23**(3), 177–186 (2004), http://dx.doi.org/10.3969/j.issn.1001-4810.2004.03.002.

8. E. A. Cloutis et al., "Detection and discrimination of sulfate minerals using reflectance spectroscopy," *Icarus* **184**(1), 121–157 (2006), http://dx.doi.org/10.1016/j.icarus.2006.04.003.

9. C. Spinetti et al., "Spectral properties of volcanic materials from hyperspectral field and satellite data compared with LiDAR data at Mt. Etna," *Int. J. Appl. Earth Obs. Geoinf.* **11**(2), 142–155 (2009), http://dx.doi.org/10.1016/j.jag.2009.01.001.

10. K. Yang et al., "Characterising the hydrothermal alteration of the Broadlands–Ohaaki geothermal system, New Zealand, using short-wave infrared spectroscopy," *J. Volcanol. Geotherm. Res.* **106**(1), 53–65 (2001), http://dx.doi.org/10.1016/S0377-0273(00)00264-X.

11. A. A. Madani, "Spectral properties of carbonatized ultramafic mantle xenoliths and their host olivine basalts, Jabal Al Maqtal basin, south eastern desert, Egypt, using ASD fieldSpec spectroradiometer," *Egypt. J. Remote Sens. Space Sci.* **14**(1), 41–48 (2011), http://dx.doi.org/10.1016/j.ejrs.2011.05.001.

12. C. Biel et al., "Mineralogical, IR-spectral and geochemical monitoring of hydrothermal alteration in a deformed and metamorphosed Jurassic VMS deposit at Arroyo Rojo, Tierra delFuego, Argentina," *J. South Am. Earth Sci.* **35**, 62–73 (2012), http://dx.doi.org/10.1016/j.jsames.2011.11.005.

13. J. B. Adams, "Visible and near-infrared diffuse reflectance: spectra of pyroxenes as applied to remote sensing of solid objects in the solar system," *J. Geophys. Res.* **79**(32), 4829–4836 (1974), http://dx.doi.org/10.1029/JB079i032p04829.

14. J. B. Adams, "Interpretation of visible and near-infrared diffuse reflectance spectra of pyroxenes and other rock forming minerals," in *Infrared and Raman Spectroscopy of Lunar and Terrestrial Minerals*, C. J. Karr, Ed., pp. 91–116, Academic Press Inc., New York (1975).

15. R. G. Burns, "Origin of electronic spectra of minerals in the visible and near-infrared region," in *Remote Geochemical Analysis: Elemental and Mineralogical Composition*, C. M. Pieters and P. A. J. Englert, Eds., pp. 3–30, Cambridge University Press Inc., New York (1993).

16. F. D. van der Meer, "Analysis of spectral absorption features in hyperspectral imagery," *Int. J. Appl. Earth Obs. Geoinf.* **5**(1), 55–68 (2004), http://dx.doi.org/10.1016/j.jag.2003.09.001.

17. J. W. Aneus, "The visible region absorption spectra of rare earth minerals," *Am. Mineral.* **50**, 356–366 (1965).

18. K. Binnemans, "Lanthanides and actinides in ionic liquids," *Chem. Rev.* **107**(6), 2592–2614 (2007), http://dx.doi.org/10.1021/cr050979c.

19. L. I. Ardanova et al., "Isomorphous substitutions of rare earth elements for calcium in synthetic hydroxyapatites," *Inorg. Chem.* **49**(22), 10687–10693 (2010), http://dx.doi.org/10.1021/ic1015127.

20. J. G. Bünzli and S. V. Eliseeva, "Basics of lanthanide photophysics," in *Lanthanide Lumin* P. Hänninen and H. Härmä, Eds., pp. 1–45, Springer, Berlin Heidelberg (2011).

21. J. F. Mustard, "Chemical composition of actinolite from reflectance spectra," *Am. Mineral.* **77**, 345–358 (1992).

22. R. F. Kokaly and R. N. Clark, "Spectroscopic determination of leaf biochemistry using band-depth analysis of absorption features and stepwise multiple linear regression," *Remote Sens. Environ.* **67**(3), 267–287 (1999), http://dx.doi.org/10.1016/S0034-4257 (98)00084-4.

23. E. F. Duke, "Near-infrared spectra of muscovite, Tschermak substitution, and metamorphic reaction progress: implications for remote sensing," *Geology* **22**(7), 621–624 (1994), http:// dx.doi.org/10.1130/0091-7613(1994)022<0621:NISOMT>2.3.CO;2.

24. B. Lacaze and R. Joffre, "Extracting biochemical information from visible and near infrared reflectance spectroscopy of fresh and dried leaves," *J. Plant Physiol.* **144**(3), 277–281 (1994), http://dx.doi.org/10.1016/S0176-1617(11)81187-9.

25. E. A. Cloutis, M. J. Gaffey, and T. F. Moslow, "Characterization of minerals in oil sands by reflectance spectroscopy," *Fuel* **74**(6), 874–879 (1995), http://dx.doi.org/10.1016/0016-2361(95)00016-X.

26. K. Randolph et al., "Hyperspectral remote sensing of cyanobacteria in turbid productive water using optically active pigments, chlorophyll a and phycocyanin," *Remote Sens. Environ.* **112**(11), 4009–4019 (2008), http://dx.doi.org/10.1016/j.rse.2008.06.002.

27. J. A. Senna, C. R. S. Filho, and R. S. Angelica, "Characterization of clays used in the ceramic manufacturing industry by reflectance spectroscopy: an experiment in the Sao Simao ball-clay deposit," *Appl. Clay Sci.* **41**(1), 85–98 (2008), http://dx.doi.org/10 .1016/j.clay.2007.10.004.

28. A. V. Bilgili et al., "Visible-near infrared reflectance spectroscopy for assessment of soil properties in a semi-arid area of Turkey," *J. Arid Environ.* **74**(2), 229–238 (2010), http://dx .doi.org/10.1016/j.jaridenv.2009.08.011.

29. T. Lammoglia and C. R. S. Filho, "Spectroscopic characterization of oils yielded from Brazilian offshore basins: potential applications of remote sensing," *Remote Sens. Environ.* **115**(10), 2525–2535 (2011), http://dx.doi.org/10.1016/j.rse.2011 .04.038.

30. K. Yang et al., "Variations in composition and abundance of white mica in the hydrothermal alteration system at Hellyer, Tasmania, as revealed by infrared reflectance spectroscopy," *J. Geochem. Explor.* **108**(2), 143–156 (2011), http://dx.doi.org/10.1016/j.gexplo.2011.01 .001.

31. C. Zhang et al., "Spectral response to varying levels of leaf pigments collected from a degraded mangrove forest," *J. Appl. Remote Sens.* **6**(1), 063501 (2012), http://dx.doi .org/10.1117/1.JRS.6.063501.

32. R. N. Clark et al., "USGS Digital Spectral Library splib06a," US Geol. Surv., Denver (2007).

33. L. C. Rowan, M. J. Kingston, and J. K. Crowley, "Spectral reflectance of carbonatites and related alkalic igneous rocks: selected samples from four north American localities," *Econ. Geol.* **81**(4), 857–871 (1986), http://dx.doi.org/10.2113/gsecongeo.81.4 .857.

34. E. Bedini, "Mapping lithology of the Sarfartoq carbonatite complex, southern west Greenland, using HyMap imaging spectrometer data," *Remote Sens. Environ.* **113**(6), 1208–1219 (2009), http://dx.doi.org/10.1016/j.rse.2009.02.007.

35. J. Silver et al., "Improvements in rare-earth-based materials," UK Patent No. 0806998.1 (2008).

36. Analytical Spectral Devices (ASD), *FieldSpec 3 User Manual*, ASD Inc., Boulder, CO (2007).

37. R. N. Clark, "Spectral properties of mixtures of montmorillonite and dark carbon grains: implications for remote sensing minerals containing chemically and physically adsorbed water," *J. Geophys. Res.* **88**(B12), 10635–10644 (1983), http://dx.doi.org/10.1029/ JB088iB12p10635.

38. R. N. Clark et al., "Imaging spectroscopy: earth and planetary remote sensing with the USGS Tetracorder and expert systems," *J. Geophys. Res.* **108**(E12), 1991–2012 (2003), http://dx.doi.org/10.1029/2002JE001847.

39. A. A. Green and M. D. Graig, "Analysis of aircraft spectrometer data with logarithmic residuals," in *Proc. Airborne Imaging Spectrometer Data Analysis*, G.Vane and A. F. H. Goetz, Eds., pp. 111–119, NASA-JPL Publication, Pasadena (1985).

40. D. J. Ketchen and C. L. Shook, "The application of cluster analysis in strategic management research: an analysis and critique," *Strategic Manage. J.* **17**(6), 441–458 (1996), http://dx.doi.org/10.1002/(ISSN)1097-0266.

Jingjing Dai earned her BS degree in geology from China University of Geosciences (Beijing), in 2004 and the MS degree in cartography and geographic information system from Institute of Remote Sensing Applications, Chinese Academy of Sciences, Beijing, in 2007. She is currently working toward the PhD degree in Faculty of Earth Sciences, China University of Geosciences (Beijing). Her research interests include reflectance spectroscopy of minerals, alteration information exaction and metallogenic prognosis using multispectral and hyperspectral remote sensing.

Denghong Wang received the BE degree in mineral resource prospecting and exploration from Chengdu University of Technology, Chengdu, China, in 1989 and the MS and the PhD degree in mineralogy from Chinese Academy of Geosciences, Beijing, in 1992 and 1995, respectively. He is currently the head of geochemistry laboratory in Institute of Mineral Resources, Chinese Academy of Geological Sciences. His research interests include regional metallogenetic rules, rare earth ores, plume magmatism, etc.

Runsheng Wang received the BS degree in geophysics from Beijing Geological College in 1967 and the MS degree in remote sensing in geology from China University of Geosciences (Beijing), in 1982. He is currently Processor of China University of Geosciences (Beijing) and China Areo Geophysical Survey and Remote Sensing Center for Land and Resources. His research interests focused on remote sensing in geology.

Zhenghui Chen received his BS degree in geology from China University of Geosciences (Wuhan), in 1995, and the MS and the PhD degree in mineralogy from Chinese Academy of Geosciences, in 2001 and 2006, respectively. His research interests include regional metallogenetic rules and metallogenic prognosis.